THE UNIVERSITY OF
WARWICK

Original citation:
McKelvey, Kim, O'Connell, Michael A. and Unwin, Patrick R.. (2013) Meniscus confined fabrication of multidimensional conducting polymer nanostructures with scanning electrochemical cell microscopy (SECCM). Chemical Communications, Volume 49 (Number 29). pp. 2986-2988. ISSN 1359-7345

Permanent WRAP url:
http://wrap.warwick.ac.uk/54253/

Copyright and reuse:
The Warwick Research Archive Portal (WRAP) makes the work of researchers of the University of Warwick available open access under the following conditions. Copyright © and all moral rights to the version of the paper presented here belong to the individual author(s) and/or other copyright owners. To the extent reasonable and practicable the material made available in WRAP has been checked for eligibility before being made available.

Copies of full items can be used for personal research or study, educational, or not-for-profit purposes without prior permission or charge. Provided that the authors, title and full bibliographic details are credited, a hyperlink and/or URL is given for the original metadata page and the content is not changed in any way.

Publisher's statement:
None

A note on versions:
The version presented here may differ from the published version or, version of record, if you wish to cite this item you are advised to consult the publisher's version. Please see the 'permanent WRAP url' above for details on accessing the published version and note that access may require a subscription.

For more information, please contact the WRAP Team at: wrap@warwick.ac.uk

warwickpublicationswrap
highlight your research

http://go.warwick.ac.uk/lib-publications

ChemComm

Dynamic Article Links ►

Cite this: DOI: 10.1039/c0xx00000x

www.rsc.org/xxxxxx

COMMUNICATION

Meniscus Confined Fabrication of Nanoscale Multidimensional Conducting Polymer Structures with Positional Feedback

Kim McKelvey,[a,b] Michael A. O'Connell[b] and Patrick R. Unwin[*,b]

Received (in XXX, XXX) Xth XXXXXXXXX 20XX, Accepted Xth XXXXXXXXX 20XX

DOI: 10.1039/b000000x

Scanning electrochemical cell microscopy (SECCM), which uses of a liquid meniscus at the end of a dual (theta) barreled pipet, is used to construct extended conducting polymer (polyaniline) structures. The SECCM technique incorporates a surface independent positional feedback mechanism, with precise control of the conducting polymer electrodeposition rate and extent.

The fabrication of individual nanoscale structures is a huge field of burgeoning interest due to numerous potential applications spanning electronic devices,[1] sensors,[2] energy[3] and lifescience technologies.[4,5] While many fabrication methods abound,[6] probe-based techniques, such as dip pen[7] and fountain pen[8] lithography, electrospinning,[9] scanning electrochemical microscopy[10,11] and meniscus-based methods[12–20] offer exciting new ways to fabricate novel structures. Previous meniscus-based fabrication techniques have made structures that have tended to make contact with a substrate at a limited number of points.[12–20] Here, we show how a dual barrel (theta) pipet, used in scanning electrochemical cell microscopy (SECCM) mode,[21-22] provides a positional feedback mechanism to control the distance between the end of the pipet and the surface. This allows extended multidimensional nanostructures to be formed and prevents pipet crash, or the meniscus becoming detached from, the surface (*vide infra*) during patterning.

For the approach herein, the meniscus at the end of the dual barrel pipet was used to deliver aniline to an electrode surface and, by adjusting the potential of the surface, localized electropolymerization could be carried out. Figure 1 A shows a scanning electron micrograph (SEM) of a typical SECCM probe, created from a borosilicate glass theta pipet, pulled using a laser puller. The pipet was filled with solution containing aniline, and supporting electrolyte (*vide infra*), and an Ag/AgCl quasi reference counter electrode (QRCE) was inserted into each barrel. An ionic conductance current, i_{Barrel}, was induced across the meniscus by applying a potential difference (V_2 in Figure 1 B), typically 100 mV, between the QRCEs. Positional feedback was achieved by oscillating the probe normal to the surface, such that the meniscus deformed at the probe oscillation frequency when it came into contact with the substrate. The resulting AC component of the conductance current were used as a set point for positional feedback of the probe.[21-22] In essence, a constant AC magnitude value maintained the distance between the end of the pipet and the surface, avoiding the probe either crashing into the surface or the meniscus becoming detached from the surface, as the surface was moved laterally under the probe.

Fig 1. SEM image of a typical SECCM probe. **B.** Schematic of the

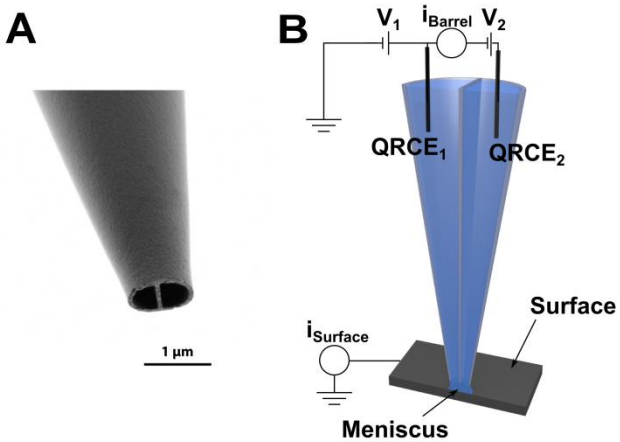

electrochemical configuration. The surface electrode was held at ground, and the surface current was measured as $i_{Surface}$. A potential, V_2, was applied between QRCEs in each barrel and the current between the barrels measured as i_{Barrel}. The QRCEs were floated, with respect to ground, by a potential V_1. Because the pipet is highly symmetric, and the contact area is small, the effective potential of the surface with respect to the QRCEs is ca. $-(V_1+V_2/2)$.

The focus herein is the conducting polymer polyaniline (PANI), which is an attractive materials to fabricate novel devices.[23,24] PANI is formed through electropolymerization, from aniline, at the interface of the meniscus and the substrate. See supplementary information Figure S1 for a characteristic cyclic voltammogram for electropolymerization from an SECCM probe on a gold substrate, which highlights an onset potential of ca. 0.8 V for electropolymerization[25] and that little detectable over-oxidation occurs at potentials where patterning was carried out. The driving force for polymerization was controllable precisely, because the substrate electrode was held at a potential of *ca.* -(V_1+V_2/2) with respect to the QRCEs (Figure 1 B).[22] In addition, the current induced by electropolymerization was measured at the substrate ($i_{Surface}$ in Figure 1 B). A galvanostatic operation mode was also assessed, in which the substrate (polymerization) current was maintained at a user-defined value by automatically adjusting the potential, V_1 in Figure 1 B, of the substrate with respect the QRCEs.

Patterns of conducting polymer can be constructed on conducting

(gold) surfaces by either: (i) controlling the position at which the liquid meniscus makes contact with the surface, held at a potential that drives the reaction; or (ii) by controlling the potential of the surface so that the reaction is 'on' or 'off' with the meniscus always in contact. To demonstrate the first approach, patterns of dots on a conducting surface (gold) were created by controlling the position of contact. Figure 2 A shows a SEM image of an array of ca. 200 nm radius PANI. The array took 641 seconds to construct, of which the meniscus was only in contact with the surface for ca. 33 seconds. The dots were made by approaching the meniscus to the surface at 50 nm s^{-1} until contact was detected, and then immediately retracting a distance of 1 µm at a speed of 200 nm s^{-1}. The probe was then moved laterally to the next dot position (at 5 µm s^{-1}) and again approached towards the surface. Throughout, the surface was held at a potential of 1.2 V with respect to the QRCEs to drive the oxidative polymerization of aniline (pH 7.2) whenever the meniscus was in contact with the surface. In this case, PANI was deposited in the non-conducting form, from the phosphate buffer (pH 7.2) solution, so that the process was self-limiting.

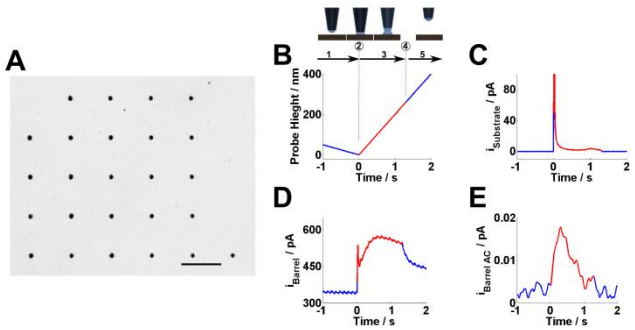

Fig 2. A. SEM of an array of 25 dots created by controlling the contact points between the liquid meniscus and the surface. Scale bar represents 5 µm. Typical SECCM responses for the formation of one dot are shown on the right with the probe position (**B**), substrate current (**C**), barrel ion-conductance current (**D**), and ac barrel current magnitude (**E**). The different stages of the probe movement are highlighted on **B: 1** probe approaches the surface; **2** meniscus comes into contact with the surface; **3** probe is immediately retracted from the surface e; **4** the meniscus detaches; **5** the probe continues to move away from the surface.

The tip position (probe height), substrate current ($i_{Surface}$) and both DC and AC components of the barrel current (i_{Barrel}) are recorded during deposition, and a typical response for each is shown in Figure 2 B through E. For clarity, the different stages of the probe movement scheme during the creation of one dot are illustrated in Figure 2 B. In the region marked 1, the tip is brought towards the surface. During this period, with the probe and meniscus in air, there is no substrate current (Figure 2 C), a constant DC current of 330 pA between the barrels (Figure 2 D) and a barely detectable AC current (Figure 2 E). When the meniscus makes contact with the substrate, point 2, there is a significant change in all 3 current measurements. First, a current flows through the substrate due to the electropolymerization process (Figure 2 C), although the surface quickly becomes passivated due to the insulating nature of the PANI deposited. There is a surge in the barrel current, largely due to an increase in the thickness of the meniscus, from a jump to contact with the surface, while the AC magnitude increases due to the periodic modulation of the meniscus.[21,22] The procedure implemented was to translate the probe away from the surface immediately at contact (Figure 2 B, region 3 – 5). The AC and DC between the barrels indicate that the meniscus maintains contact with the surface for about 200 nm and then detaches (Figure 2 B, point 4). Analysis of the substrate charge and area per dot, shown in the supplementary information, show the consistency of the dots.

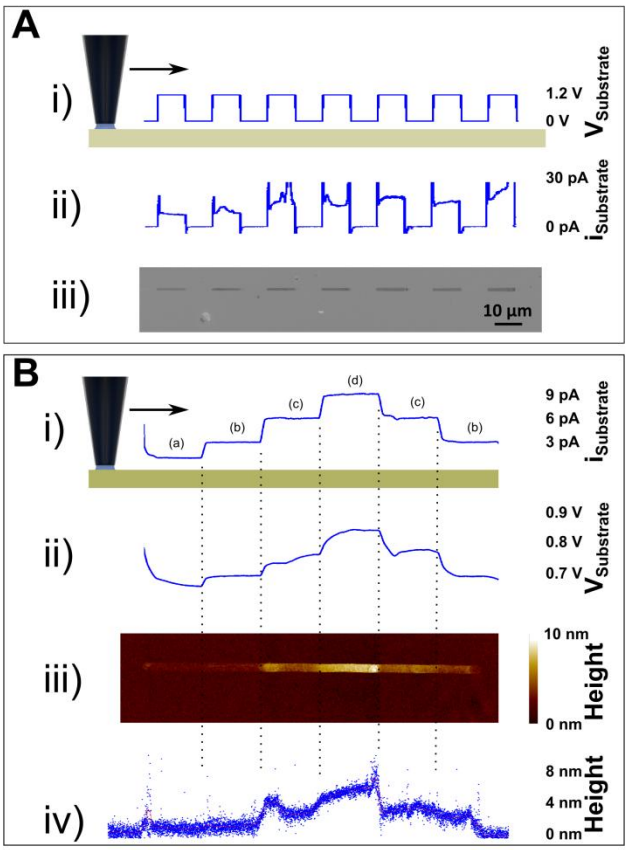

Fig 3. Patterning of PANI on a gold surface by controlling the surface potential (i) while the meniscus is scanned across surface. The substrate current (ii) indicates the magnitude of the polymerization rate as does the SEM micrograph of the resulting PANI pattern (iii). **B.** Galvanostatic control of PANI electrodeposition as a meniscus is moved, in contact, laterally across a gold surface electrode surface: (i) measured substrate current stepped through values of (a) 1 pA (b) 3 pA (c) 6 pA and (d) 9 pA and corresponding applied surface potential (ii) to drive the surface current. The AFM image of the resulting pattern (iii) and cross section height (iv) qualitatively reflects the different applied substrate currents.

Next, patterns were produced by the second method, moving the meniscus laterally across the surface while controlling the effective potential of the substrate surface, $V_{Substrate}$, with respect to the QRCEs in the barrels of the probe, by changing V_1, while V_2 was fixed, as is demonstrated in Figure 3 A(i). A 1 µm diameter probe was used, and for this study, and all following studies, PANI was deposited in its conducting form from a pH 1.6 aniline solution. The probe was moved laterally over the substrate, with the meniscus kept in contact with the surface throughout (see supporting information Figure S3 which shows a strong AC current signal used for positioning). A substrate current, of ca. 20 - 30 pA (Figure 3 A(ii)), was measured when the potential of the surface (1.2 V) was sufficient to drive the formation of PANI, while no current was measured when it was not (0 V). The SEM image (Figure 3 A(iii)) confirms the

This journal is © The Royal Society of Chemistry [year]

oxidative polymerization of aniline, producing PANI, only occurs when the potential of the surface was 1.2 V with respect to the QRCEs. The result is a well-defined 'dashed line' with a width of ca 1 µm.

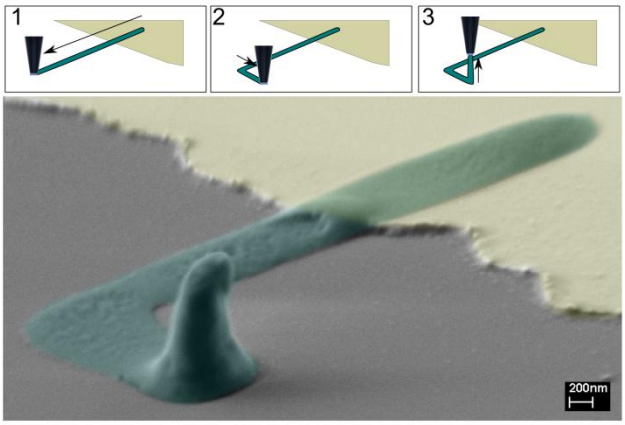

Fig 4. SEM (false color) of a three dimensional PANI structure (green) created on a conducting (gold) and non-conducting (grey) surface. The probe movement steps are shown as: 1 the lateral movement from a conducting substrate and over an insulating substrate; 2 the change in lateral movement direction on an insulating substrate; and 3 moving the probe away from the surface.

As an alternative to potentiostatic deposition, a galvanostatic approach was used. This procedure and typical results are illustrated in Figure 3 B showing: (i) the current measured at the substrate; (ii) potential required to maintain the prescribed current; (iii) an AFM image of the resulting pattern; and (iv) the average cross-sectional height of the deposited line deduced from the AFM image. As a probe was moved laterally across the surface (at 300 nm s^{-1}) a user defined substrate current was maintained for 5 µm by adjusting the potential of the surface (V_1). A surface current of 1 pA generated a 0.9 ± 0.6 nm thick layer of PANI, while a surface current of 9 pA deposited a 5 ± 0.7 nm thick layer of PANI. This demonstrates that it is possible to move a meniscus based probe across a surface, using one feedback loop to control the contact of the meniscus with the surface, while another feedback loops controls the quantity of PANI deposited on the surface.

Finally, we show the power of using a dual barrel pipet, with positional feedback, to construct multidimensional structures. Figure 4 shows a three-dimensional structure that started on a conducting substrate but then moved out across an insulating substrate (shown in schematic 1 of Figure 4). The laterally direction of the probe was then changed to turn a 1-D nanowire into a 2-D pattern on the insulating substrate (shown in schematic 2 of Figure 4). This highlights that good electrical contact is maintained between the polymeric nanowire and the gold contact, even when the wire is on an insulating substrate. Finally, a three-dimensional structure was created by holding the probe still and following, using the feedback response, the growing tower (shown in schematic 3 of Figure 4).

In conclusion, we have demonstrated the use of a dual barrel SECCM-based meniscus method to create multidimensional PANI nanostructures on conducting substrates, across insulating (inert) areas of a surface, and ultimately to produce 3D structures. Given the wide range of materials that can be created by electrodeposition, we expect the SECCM nanofabrication technique to have a wide applications, particularly for the creation of novel nanodevices and sensing elements that maybe difficult to construct with other techniques.

We thank Massimo Peruffo, Aleix Güell, Stanley Lai and Anisha Patel for useful discussions, and Aleix Güell for substrate preparation. We thank the EPSRC and MOAC for a studentship to K.M. P.R.U acknowledges support from a European Research Council Advanced Investigator Grant (ERC-2009-AdG247143 Quantif). Some of the equipment used in this work was obtained through the Science City Advanced Materials project with support from Advantage West Midlands and the European Regional Development Fund.

Notes and references

[a]*MOAC Doctoral Training Centre and* [b]*Department of Chemistry, University of Warwick, Coventry, UK. Fax: +44 (0)2476 524112; Tel: +44 (0)24 76 523653; E-mail: p.r.unwin@warwick.ac.uk*

† Electronic Supplementary Information (ESI) available: [details of any supplementary information available should be included here]. See DOI: 10.1039/b000000x/

1 Wang, Z. L. Adv. Mater. 2012, 24, 4632–46.
2 Penner, R. M. Ann. Rev. Anal. Chem. 2012, 5, 461–85.
3 Hochbaum, A. I.; Chen, R.; Delgado, R. D.; Liang, W.; Garnett, E. C.; Najarian, M.; Majumdar, A.; Yang, P. Nature 2008, 451, 163–7.
4 Xie, C.; Lin, Z.; Hanson, L.; Cui, Y.; Cui, B. Nat. Nanotechnol. 2012, 7, 185–90.
5 Shalek, A. K.; Robinson, J. T.; Karp, E. S.; Lee, J. S.; Ahn, D.-R.; Yoon, M.-H.; Sutton, A.; Jorgolli, M.; Gertner, R. S.; Gujral, T. S.; MacBeath, G.; Yang, E. G.; Park, H. Proc. Natl. Acad. Sci. USA 2010, 107, 1870–5.
6 Xia, Y.; Rogers, J. A.; Paul, K. E.; Whitesides, G. M. Chem. Rev. 1999, 99, 1823–48.
7 Salaita, K.; Wang, Y.; Mirkin, C. A. Nat. Nanotechnol. 2007, 2, 145–55.
8 Kim, K.-H.; Moldovan, N.; Espinosa, H. D. Small 2005, 1, 632–5.
9 Sun, D.; Chang, C.; Li, S.; Lin, L. Nano Lett. 2006, 6, 839–42.
10 Zhou, J.; Wipf, D. O. J. Electrochem. Soc. 1997, 144, 1202–7.
11 Sheffer, M.; Mandler, D. J. Electrochem. Soc. 1995, 142, 82–4.
12 Grilli, S.; Coppola, S.; Vespini, V.; Merola, F.; Finizio, A.; Ferraro, P. Proc. Natl. Acad. Sci. USA 2011, 108, 15106–11.
13 Hu, J.; Yu, M.-F. Science 2010, 329, 313–6.
14 Kim, J. T.; Seol, S. K.; Pyo, J.; Lee, J. S.; Je, J. H.; Margaritondo, G. Adv. Mater. 2011, 23, 1968–70.
15 Laslau, C.; Williams, D. E.; Kannan, B.; Travas-Sejdic, J. Adv. Funct. Mater. 2011, 21, 4607–16.
16 Laslau, C.; Williams, D. E.; Travas-Sejdic, J. Prog. Polym. Sci. 2012, 37, 1177–91.
17 Yang, D.; Han, L.; Yang, Y.; Zhao, L.-B.; Zong, C.; Huang, Y.-F.; Zhan, D.; Tian, Z.-Q. Angew. Chem. Int. Edit. 2011, 50, 8679–82.
18 Zhan, D.; Yang, D.; Zhu, Y.; Wu, X.; Tian, Z.-Q. Chem. Comm. 2012, 48, 11449–51.
19 Rodolfa, K. T.; Bruckbauer, A.; Zhou, D.; Schevchuk, A. I.; Korchev, Y. E.; Klenerman, D. Nano Lett. 2006, 6, 252–7.
20 Rodolfa, K. T.; Bruckbauer, A.; Zhou, D.; Korchev, Y. E.; Klenerman, D. Angew. Chem. Int. Edit. 2005, 44, 6854–9.
21 Ebejer, N.; Schnippering, M.; Colburn, A. W.; Edwards, M. A.; Unwin, P. R. Anal. Chem. 2010, 82, 9141–5.
22 Snowden, M. E.; Güell, A. G.; Lai, S. C. S.; McKelvey, K.; Ebejer, N.; O'Connell, M. A.; Colburn, A. W.; Unwin, P. R. Anal. Chem. 2012, 84, 2483–91.
23 Zhang, D.; Wang, Y. Mat. Sci. Eng. B 2006, 134, 9–19.
24 Chen, D.; Lei, S.; Chen, Y. Sensors 2011, 11, 6509–16.
25 Gospodinova, N.; Terlemezyan, L. Prog. Polym. Sci. 1998, 23, 1443–84.